© 2015. Published by The Company of Biologists Ltd | Journal of Cell Science (2015) 128, 4366-4379 doi:10.1242/jcs.173518

RESEARCH ARTICLE

Carcinoma cells induce lumen filling and EMT in epithelial cells through soluble E-cadherin-mediated activation of EGFR

Pratima U. Patil[1,2], Julia D'Ambrosio[2], Landon J. Inge[3], Robert W. Mason[2] and Ayyappan K. Rajasekaran[1,4,*]

ABSTRACT

In epithelial cancers, carcinoma cells coexist with normal cells. Although it is known that the tumor microenvironment (TME) plays a pivotal role in cancer progression, it is not completely understood how the tumor influences adjacent normal epithelial cells. In this study, a three-dimensional co-culture system comprising non-transformed epithelial cells (MDCK) and transformed carcinoma cells (MSV-MDCK) was used to demonstrate that carcinoma cells sequentially induce preneoplastic lumen filling and epithelial–mesenchymal transition (EMT) in epithelial cysts. MMP-9 secreted by carcinoma cells cleaves cellular E-cadherin (encoded by *CDH1*) from epithelial cells to generate soluble E-cadherin (sE-cad), a pro-oncogenic protein. We show that sE-cad induces EGFR activation, resulting in lumen filling in MDCK cysts. Long-term sE-cad treatment induced EMT. sE-cad caused lumen filling by induction of the ERK signaling pathway and triggered EMT through the sustained activation of the AKT pathway. Although it is known that sE-cad induces MMP-9 release and consequent EGFR activation in tumor cells, our results, for the first time, demonstrate that carcinoma cells can induce sE-cad shedding in adjacent epithelial cells, which leads to EGFR activation and the eventual transdifferentiation of the normal epithelial cells.

KEY WORDS: EGFR, MMP-9, Soluble E-cadherin, Transdifferentiation

INTRODUCTION

Bidirectional communication between tumor cells and the microenvironment plays a crucial role in driving tumor progression. The tumor microenvironment (TME) is comprised of a heterogeneous population of cells, including stromal cells, adjacent normal cells, fibroblasts, infiltrating immune cells and angiogenic vascular cells, and secretions from these cells such as growth factors, cytokines and extracellular matrix (ECM) (Hanahan and Coussens, 2012). During the initial stages of carcinogenesis, the surrounding normal epithelial cells and other microenvironment components are anti-tumorigenic as they block transformed cell proliferation and survival (Hogan et al., 2011; Kajita et al., 2010; Toillon et al., 2002). However, once tumor cells multiply and override this self-defense mechanism, they modify and cause the evolution of the non-transformed cell types to participate in tumor progression (Ivers et al., 2014). For instance, normal prostate epithelial cells can induce intraepithelial neoplasia in mice when co-injected with carcinoma-associated fibroblasts (CAFs) but not when co-injected with normal fibroblasts, suggesting alteration of fibroblasts by tumor cells (Olumi et al., 1999). Similarly CAFs from breast cancer tissue induce EMT and enhance the metastatic potential of both premalignant and malignant breast epithelial cells, unlike normal fibroblasts, which suppress metastasis (Orimo et al., 2005). Although some aspects of the TME, such as ECM remodeling and tumor angiogenesis are well studied, the interaction between tumor cells and the adjacent epithelium is poorly understood.

Epithelial cells in the tissues reorganize themselves to form tubular networks and cyst-like spheroids (Zegers et al., 2003). Spherical epithelial cysts are the building blocks of glandular organs and are characterized by a hollow lumen with apical–basal polarity (Bryant and Mostov, 2008). An intact, hollow lumen formed by selective apoptosis of centrally located cells in the cyst is crucial for proper control and function of epithelial tissues (Debnath et al., 2002). However, abnormal pathophysiological conditions cause lesions in the lumen, resulting in the formation of multiple lumens and, finally, filling of the luminal space by cells. Filling of the lumen is a salient feature of early pre-invasive stages of epithelial cancers (Debnath and Brugge, 2005). Several carcinomas such as breast, kidney and prostate carcinomas display lumen filling during their early stages (Debnath and Brugge, 2005). Lumen filling is followed by epithelial to mesenchymal transition (EMT), a transdifferentiation process, which facilitates invasion and the metastatic potential of carcinoma cells (Tiwari et al., 2012).

A key event observed during epithelial-derived carcinogenesis is the downregulation of E-cadherin (also known as CDH1), a Ca^{2+}-dependent cell adhesion molecule located in the adherens junction and along the basolateral surface of epithelial cells (Gumbiner et al., 1988; Takeichi, 1991). One of the mechanisms by which tumor cells downregulate E-cadherin is by the proteolytic cleavage of its extracellular domain. Matrix metalloproteinase (MMP)-9, one of the proteases present in the extracellular environment, cleaves the ectodomain of membrane-bound E-cadherin at the MMP cleavage site between amino acids Leu581 and Ser582 to generate a 80-kDa fragment referred to as soluble E-cadherin (sE-cad) (De Wever et al., 2007; Maretzky et al., 2005). MMP-9 levels are elevated in several cancers, and this enzyme appears to be involved in tumor cell initiation and progression, metastatic ability and genetic instability (Farina and Mackay, 2014).

Significantly elevated sE-cad levels have been observed in the sera and urine of cancer patients diagnosed with a variety of cancers. Increased circulating levels of sE-cad are indicative of histopathological grade, metastasis recurrence and poor prognosis (Chan et al., 2003; De Wever et al., 2007; Katayama et al., 1994). In human skin, breast, prostate and ovarian cancer cells, the pathophysiological consequences of sE-cad activity include enhanced tumor cell migration and invasion, induction of pro-invasive MMPs and increased cell signaling, all of which ultimately

[1]Department of Biological Sciences, University of Delaware, Newark, DE 19716, USA. [2]Nemours Center for Childhood Cancer Research, Department of Biomedical Research, Alfred I. duPont Hospital for Children, Wilmington, DE 19803, USA. [3]Thoracic and Esophageal disease, Norton Thoracic Institute, St. Joseph's Hospital and Medical Center, Phoenix, AZ 85013, USA. [4]Therapy Architects, LLC, 2700, Silverside Road, Wilmington, DE 19810, USA.

*Author for correspondence (raj@therapyarchitects.com)

Received 28 April 2015; Accepted 13 October 2015

Journal of Cell Science (2015) 128, 4366-4379 doi:10.1242/jcs.173518

promote tumor progression (Brouxhon et al., 2007, 2014a, 2013b; David and Rajasekaran, 2012; Noe et al., 2001; Symowicz et al., 2007; Zuo et al., 2011). We have previously demonstrated that sE-cad acts as a survival factor and prevents apoptosis in normal epithelial cells (Inge et al., 2011). However, it is not known whether the sE-cad present in the TME impacts normal tissue architecture.

In tumor cells, sE-cad mediates its pro-oncogenic effects predominantly by activating the epidermal growth factor receptor (EGFR) pathway. In MCF-7 breast cancer cells sE-cad complexes with the HER2 and HER3 receptors (also known as ERBB2 and ERBB3, respectively) of the EGFR family, resulting in enhanced tumor cell migration and invasion (Najy et al., 2008). In squamous cell carcinoma cells, sE-cad contributes to skin carcinogenesis through association with HER1–HER3 and insulin-like growth factor-1 receptor (IGF-1R), resulting in activation of the downstream MAPK–PI3K–AKT–mTOR pathway [i.e. the pathway mediated by mitogen-activated protein kinases, phosphatidylinositol 3-kinase (PI3K), AKT and mammalian target of rapamycin (mTOR)] and inhibitor of apoptosis signaling (Brouxhon et al., 2014a). An E-cadherin-ectodomain-specific monoclonal antibody, Decma-1, has been found to suppress tumor growth by downregulation of levels of EGFR family members and downregulation of components of the MAPK–PI3K–AKT–mTOR pathways resulting in apoptosis (Brouxhon et al., 2013a). However, it is not known whether elevated circulating levels of sE-cad can also deregulate cell signaling events in normal epithelial cells.

In this study, we addressed the question of how tumor cells interact and alter adjacent normal epithelial cells. Using a three-dimensional (3D) co-culture system comprised of non-transformed Madin–Darby canine kidney (MDCK) epithelial cells to represent normal epithelial cells and Moloney sarcoma virus transformed MDCK (MSV-MDCK) as carcinoma cells, we demonstrate that carcinoma cells sequentially induce pre-neoplastic lumen filling and EMT in MDCK cysts. We show that carcinoma cells secrete MMP-9, which cleaves E-cadherin from the basolateral surface of MDCK cells to generate sE-cad. sE-cad in turn induces lumen filling and EMT through activation of EGFR and its downstream ERK and AKT pathways. These studies demonstrate that carcinoma cells utilize normal epithelial cells to generate a pro-oncogenic peptide, sE-cad, which facilitates transdifferentiation of normal epithelial cells.

RESULTS

Co-culture of carcinoma cells with MDCK cysts disrupts luminal architecture

To investigate how invasive carcinoma cells influence adjacent normal epithelial cells, MDCK cysts (red) were co-cultured with MSV-MDCK cells (green). After 72 h, MDCK cells formed polarized cysts with hollow lumens (Fig. 1A). At this time point MSV-MDCK cells were added and co-culture established. At 4 and 8 h after addition of these cells the MDCK cysts were deformed and revealed multiple lumens (Fig. 1B,C), whereas after 24 h of co-culture the lumen was filled with cells (Fig. 1D). Quantification revealed that in co-culture conditions, 80% of the cysts showed a filled lumen (Fig. 1G). Direct contact of MDCK cysts through extension of filopodia-like structures from MSV-MDCK cells were obvious in some cases (Fig. 1D, arrow). Interestingly, MDCK cysts that were not in direct contact with MSV-MDCK cells also showed a filled lumen suggesting that a soluble component produced in co-culture is involved in the induction of lumen filling in MDCK cysts. Consistent with this hypothesis, conditioned medium collected from MSV-MDCK cells induced lumen filling in ~80% of MDCK cysts (Fig. 1F,H). These results indicate that carcinoma cells disrupt epithelial luminal architecture by secreting a soluble factor.

MSV-MDCK cells induce shedding of sE-cad from MDCK cysts in an MMP-9-dependent manner

MMP-9 secreted by invasive carcinoma cells has been shown to facilitate invasion by modification of the ECM (Farina and Mackay, 2014). Therefore, we measured the levels of MMPs in conditioned medium derived from co-culture. MDCK cysts in co-culture showed a 2.7-fold increase in total MMP-9 levels compared to cysts grown alone (Fig. 2A). Quantification of active MMP-9 using gelatin

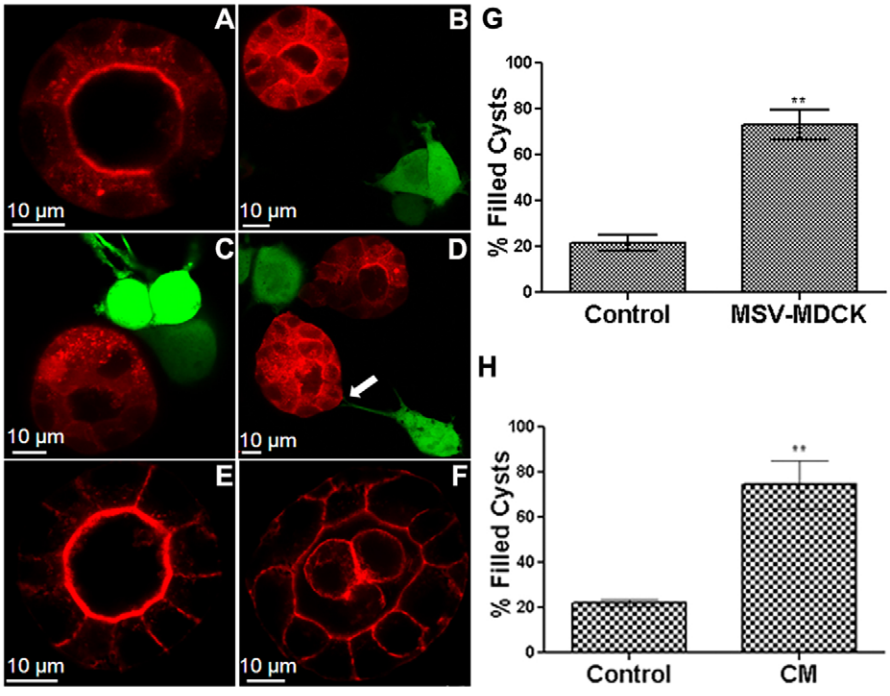

Fig. 1. Co-culture of carcinoma cells with MDCK cysts disrupt luminal architecture. MDCK–RFP cysts (red) were formed by culturing the cells for 72 h in Matrigel™ (A). MSV-MDCK–GFP cells (green) were then added in co-cultures and imaged after 4 h (B), 8 h (C) and 24 h (D). The arrow in D points to a filopodium from an MSV-MDCK cell contacting a cyst. Control cysts were cultured alone for an additional 24 h (E). MDCK–RFP cysts were treated with conditioned medium (CM) from MSV-MDCK cells for 24 h (F). Lumen-filled cysts in three independent experiments were counted and compared to controls after 24 h in the co-culture (G) or after exposure to the conditioned medium from tumor cells for 24 h (H). Results are mean±s.e.m. $^{**}P<0.005$ (Student's *t*-test).

Journal of Cell Science (2015) 128, 4366-4379 doi:10.1242/jcs.173518

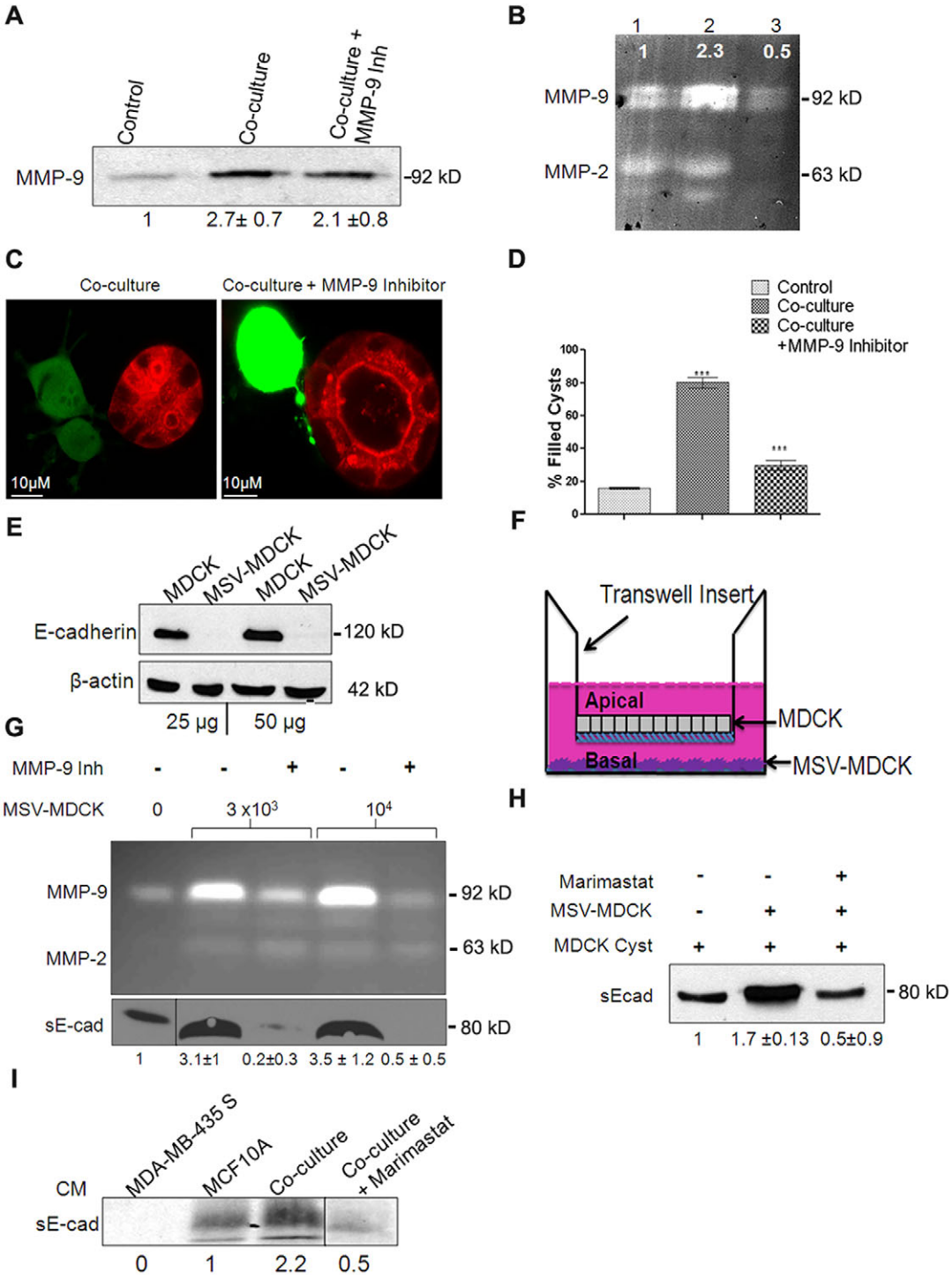

Fig. 2. Conditioned medium from co-culture contains active MMP-9, which is crucial for lumen filling and mediates sE-cad shedding in MDCK cysts. (A) Representative immunoblot from three independent experiments showing MMP-9 levels in the supernatant from MDCK 3D cultures. Quantification data are shown underneath the blot and are expressed as mean±s.e.m. from three independent experiments. (B) Representative zymogram from three independent experiments showing MMP-9 activity. Lane 1, MDCK control; lane 2, co-culture; lane 3, co-culture+10 μM MMP-9 inhibitor. The intensity of MMP-9 bands normalized to control is shown. (C) Confocal images showing co-culture in presence and absence of 10 μM MMP-9 inhibitor after 24 h treatment. Note the absence of lumen filling with MMP-9 inhibition (right panel). (D) Quantification of lumen filling in MDCK cysts in the presence and absence of MMP-9 inhibitor from an average of three independent experiments. Results are mean±s.e.m. ***P<0.0001 (Student's t-test). (E) Representative immunoblot from two independent experiments showing E-cadherin levels in MDCK and MSV-MDCK cells. β-actin is used as a loading control. (F) Diagrammatic representation of the Transwell co-culture system. (G) Top panel, zymogram showing MMP-9 activity in the conditioned medium from the bottom chamber of the Transwell. A dose-dependent increase in MMP-9 levels with increasing number of MSV-MDCK cells in the bottom chamber was observed. 10 μM of MMP-9 inhibitor was used to block MMP-9 activity in the bottom chamber. Bottom panel, immunoblot showing sE-cad levels in the conditioned medium (CM) in the bottom chamber of the Transwell. (H) Immunoblot showing increased sE-cad levels in the co-culture conditioned medium. Note that in the presence of MMP-9 inhibitor, sE-cad levels were reduced. (I) Immunoblot showing sE-cad levels in the bottom chamber of a Transwell assay consisting of MCF10A and MDA-MB435S cell lines. Quantification data are shown as mean±s.e.m. from three experiments underneath the blots for A,G,H and I.

Journal of Cell Science (2015) 128, 4366-4379 doi:10.1242/jcs.173518

zymography revealed a 2.3-fold increase in the co-culture conditioned medium. Addition of CAS-1177749, an MMP-9 inhibitor, substantially reduced the level of active MMP-9 (Fig. 2B), but the total MMP-9 protein level was not altered (Fig. 2A). Treatment of MDCK–MSV-MDCK co-cultures with MMP-9 inhibitor prevented lumen filling (Fig. 2C). Quantification of these results indicated that MMP-9 inhibitor treatment was effective in blocking lumen filling in ∼70% of the cysts in co-culture (Fig. 2D).

MMP-9 cleaves the E-cadherin extracellular domain to produce a soluble fragment known as sE-cad (Symowicz et al., 2007). Immunoblot analysis revealed that MSV-MDCK cells lack E-cadherin expression (Fig. 2E; Behrens et al., 1989) and, therefore, these cells are unlikely to be a major source of sE-cad. This led us to hypothesize that under co-culture conditions, MMP-9 produced by MSV-MDCK cells cleaves cell surface E-cadherin from MDCK cells to generate sE-cad.

Two independent assays were used to demonstrate that sE-cad is produced from MDCK cells. First, MDCK cells were grown on transwell filters to form polarized monolayers with functional tight junctions [transepithelial resistance (TER) >250 Ω/cm^2]. MSV-MDCK cells were co-cultured in the lower chamber, facing the basolateral side of the polarized MDCK monolayer (Fig. 2F). Active MMP-9 and sE-cad levels in the media from the apical and basolateral chambers were determined using gelatin zymography and immunoblot analyses, respectively. MMP-9 and sE-cad were not detected in the conditioned medium collected from the apical chamber. MMP-9 activity in the basolateral chamber was six times higher in conditioned medium from co-cultures compared to MDCK cells grown alone. There was a dose-dependent increase in MMP-9 levels with increasing numbers of MSV-MDCK cells in the bottom chamber. In the presence of an inhibitor of MMP-9, activity was substantially reduced (Fig. 2G). Immunoblot analysis revealed a 2-fold increase of sE-cad levels in co-culture conditioned medium (Fig. 2G, bottom panel). We then evaluated sE-cad shedding using our 3D-culture system. In this assay, MSV-MDCK cells were co-cultured with MDCK cysts, and the levels of sE-cad in the conditioned medium were compared to that from MDCK cysts grown alone. There was a 1.9-fold increase in sE-cad levels in the conditioned medium of MDCK cysts challenged with MSV-MDCK cells compared to that of control. MMP-9 inhibition reduced sE-cad levels by 75% (Fig. 2H). Taken together, these results demonstrate that MSV-MDCK cells induce MMP-9-mediated sE-cad shedding from the basolateral surface of MDCK cells.

To demonstrate that tumor-cell-secreted MMPs induce sE-cad shedding in other epithelial cells, a transwell co-culture assay consisting of human breast epithelial cells, MCF10A and MDA-MB-435S (E-cadherin-negative invasive human breast cancer cells) were used. The data demonstrate that MMP released from MDA-MB43S cleaved E-cadherin from MCF10A cells to generate sE-cad. Compared to MCF10A cells grown alone, co-culture conditioned medium from the basal chamber revealed a 2.2-fold increase in sE-cad levels (Fig. 2I). This processing was blocked by Marimastat, a broad spectrum MMP inhibitor. These data confirm that MMPs released from human tumor cells generate sE-cad from human epithelial cells as observed in the MDCK co-culture system.

sE-cad is necessary to induce lumen filling in MDCK cysts

Lumen filling might be induced by multiple factors present in the conditioned medium. To determine whether sE-cad is crucial for the induction of lumen filling, two independent assays were performed. First, we tested the effect of purified sE-cad on lumen filling. As shown in Fig. 3A,B, recombinant purified sE-cad exogenously added to MDCK cysts induced lumen filling. Next, to demonstrate that sE-cad is involved in the induction of lumen filling induced by conditioned medium, a sE-cad immunodepletion assay was utilized. In this assay, sE-cad was removed from the co-culture conditioned medium by immunoprecipitation using an antibody against the extracellular domain of E-cadherin. sE-cad depletion in the conditioned medium was confirmed by immunoblotting (Fig. 3C). sE-cad-depleted conditioned medium failed to induce lumen filling in the MDCK cysts, whereas untreated conditioned medium induced lumen filling in 80% of the cysts (Fig. 3D,E). These results demonstrate that sE-cad is a crucial soluble factor involved in lumen filling in MDCK cysts. It also indicates that lumen filling induced by MSV-MDCK cells is mediated by sE-cad.

MSV-MDCK cells mediate lumen filling through activation of EGFR

Activation of the EGFR has been implicated in sE-cad-mediated proliferation, migration and invasion effects (Brouxhon et al., 2007, 2013a; Inge et al., 2011; Maretzky et al., 2005; Najy et al., 2008; Noe et al., 2001). We therefore hypothesized that the induction of lumen filling by MSV-MDCK cell co-culture is mediated by the activation of EGFR signaling in MDCK cysts. The phosphorylation of EGFR in MDCK cysts following co-culture with MSV-MDCK cells or conditioned medium was visualized using immunofluorescence and confocal microscopy. As shown in Fig. 4A, co-culture of MDCK cysts with MSV-MDCK cells and conditioned medium disrupted luminal architecture and enhanced EGFR phosphorylation at the Tyr1068 which could be blocked by the EGFR inhibitor CL-387,785. Stimulation with EGF also resulted in EGFR phosphorylation and disruption of the hollow luminal architecture in MDCK cysts. Consistent with the immunofluorescence data, a quantifiable immunoblot analysis showed a 1.5- and 2-fold increase in the phosphorylation of EGFR in the co-culture and conditioned medium conditions, respectively. This phosphorylation was blocked by the EGFR inhibitor (Fig. 4B,D). Addition of purified sE-cad to MDCK cysts induced a 3-fold increase in EGFR phosphorylation, which was also inhibited by CL-387,785 (Fig. 4A,B,D). Immunoblot analysis did not reveal substantial changes in the phosphorylation of other EGFR tyrosine residues at 1173, 1045 and 1086.

sE-cad is reported to associate with the HER2–HER3 receptor of the EGFR family in breast cancer cells and also interacts with EGFR in squamous skin cancer cells (Brouxhon et al., 2007; Najy et al., 2008). To investigate whether sE-cad acts as a ligand for EGFR in MDCK epithelial cells, co-immunoprecipitation analysis was done to detect association between sE-cad and phosphorylated EGFR (pEGFR) in sE-cad-treated MDCK cells (Fig. S1A). The recombinant sE-cad used has a Myc tag at its N-terminus. To prevent pulling down cellular E-cadherin along with sE-cad, anti-Myc antibody was used. Co-immunoprecipitation analysis showed an association between phosphorylated EGFR and sE-cad in MDCK cells, indicating that sE-cad binds to the EGF receptor in MDCK cells.

Furthermore, the mechanism by which sE-cad activates EGFR was investigated using a cell surface biotinylation assay. Cell surface localization of EGFR is crucial for its activation. Internalization of EGFR following ligand binding functions as a negative regulatory mechanism, and prolonged membrane signaling of EGFR is associated with oncogenesis (Tomas et al., 2014). Therefore, cell surface levels of EGFR were compared following EGF and sE-cad treatment. In this assay, a cleavable biotin was used for cell surface biotinylation. Following biotinylation, cells were

Journal of Cell Science (2015) 128, 4366-4379 doi:10.1242/jcs.173518

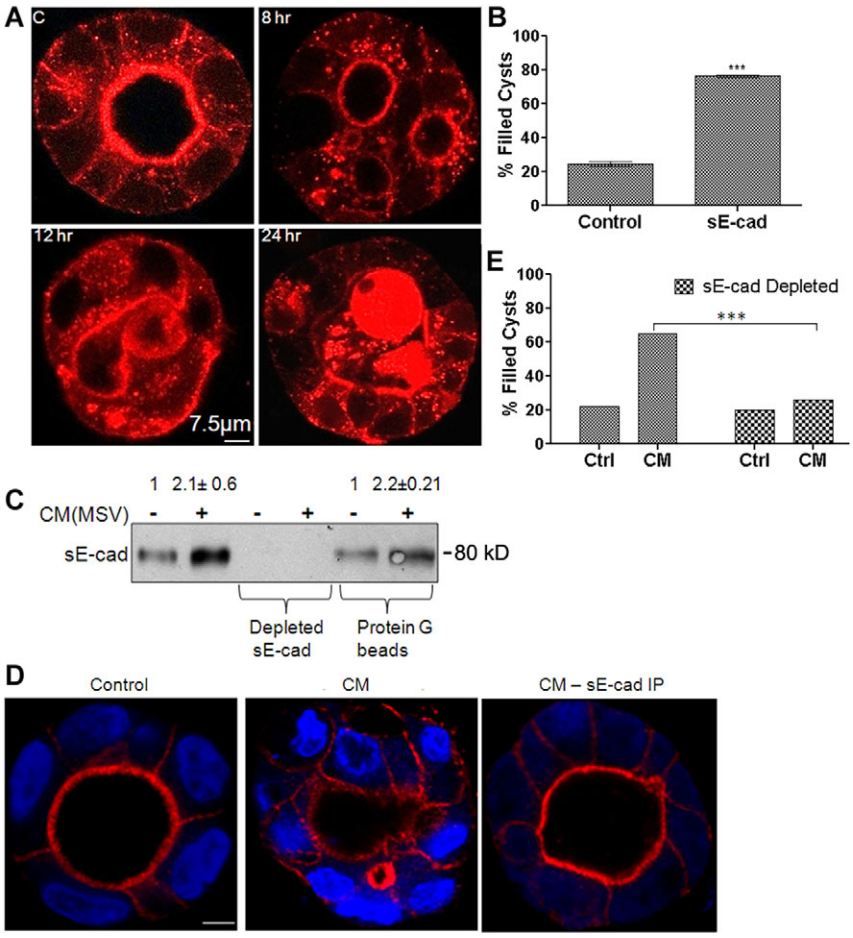

Fig. 3. sE-cad is necessary for induction of lumen filling in MDCK cysts. (A) Representative confocal images showing lumen filling and disrupted epithelial architecture induced by 10 µg/ml purified sE-cad over 24 h. (B) Quantification of lumen filling from three independent experiments. Results are mean±s.e.m. ***P<0.0001 (Student's t-test). (C) Immunoblot showing sE-cad levels in the conditioned medium before and after immunodepletion of sE-cad. Quantification data represent mean±s.e.m. from three independent experiments. Note that the immunodepleted sE-cad is bound to Protein G beads. (D) Representative confocal images of control cysts, conditioned medium (CM)-treated cysts and cysts treated with sE-cad-depleted conditioned medium. Cysts were stained for actin (red) and TOPRO-3 (nuclear marker, blue). (E) Quantification of lumen-filled cysts in presence of conditioned medium and sE-cad-depleted conditioned medium. Results are mean±s.e.m. for B,E and the blot shown in C. ***P<0.001 (Student's t-test).

treated with either EGF or sE-cad and incubated at 37°C to allow internalization. At the indicated time intervals, cells were treated with a reducing agent to remove the biotin from the cell surface. The biotinylated internalized proteins are protected from the reducing agent and can be visualized on an immunoblot. The lysates were affinity precipitated using streptavidin beads and immunoblotted with anti-EGFR and anti-E-cadherin antibodies. As shown in Fig. S1B, treatment with EGF resulted in the internalization of EGFR. In contrast, sE-cad-treated cells did not reveal substantial internalization of EGFR (Fig. S1B). Calculation of EGFR cell surface levels indicated that 64% and 71% of the total EGFR remained at the cell surface after 30 and 60 min of sE-cad treatment compared to 25% and 29% in EGF-treated cells (Fig. S1C). In addition, we found that EGF induced internalization of E-cadherin, whereas E-cadherin was not internalized following sE-cad treatment (Fig. S1B). Taken together, these findings indicate that sE-cad is involved in the activation of EGFR.

Depending on the phosphorylation pattern at the different tyrosine sites of EGFR, distinct downstream signaling pathways are activated (Chattopadhyay et al., 1999; Sturla et al., 2005; Yarden, 2001). We demonstrated that EGF, sE-cad, conditioned medium and MSV-MDCK induced phosphorylation of EGFR at Tyr1068. Tyr1068 phosphorylation results in receptor dimerization, recruitment of Grb2 and subsequent activation of the AKT and ERK1 and ERK2 (ERK1/2, also known as MAPK3 and MAPK1, respectively) signaling pathway (Rojas et al., 1996). To determine whether the Grb2 adaptor protein binds EGFR Tyr1068, conditioned medium or sE-cad-treated cyst lysates were immunoprecipitated with anti-Grb2 antibody and blotted using an anti-pEGFR-1068 antibody. Treatment with conditioned medium or purified sE-cad showed an enhanced association of pEGFR with Grb2 in MDCK cells (Fig. 4C). At 4 h there was a 1.7 to 2-fold increase in association of pEGFR with Grb2. Consistent with the activation of EGFR, downstream AKT (detected using a pan-AKT antibody) and ERK1/2 signaling was activated after co-culture or treatment with conditioned medium and sE-cad (Fig. 4B,D). Taken together, these results demonstrate that lumen filling induced by MSV-MDCK cells involves sE-cad shedding and activation of EGFR and subsequent downstream ERK1/2 and AKT signaling pathways in MDCK cysts.

Lumen filling is a consequence of increased survival and proliferation mediated by the MEK–ERK pathway

To determine whether activation of ERK1/2 and AKT signaling mediated by sE-cad results in increased cell proliferation or an inhibition of apoptosis leading to lumen filling, we analyzed expression levels of cell proliferation markers and anti-apoptotic markers. Ki67 (also known as MKI67) is a nuclear protein associated with cell proliferation (Scholzen and Gerdes, 2000). Confocal microscopy showed that MDCK cysts treated with conditioned medium or sE-cad for 48 h had enhanced Ki67 nuclear staining, consistent with increased proliferation (Fig. 5A). Immunofluorescence analysis revealed enhanced expression of Bcl2, an anti-apoptotic marker in sE-cad- and conditioned medium-treated cysts compared to their respective controls (Fig. 5A). Immunoblot analysis of Ki67 and cyclin D1, a second cell proliferation marker, and Bcl2 confirmed enhanced expression in sE-cad- or conditioned-medium-treated cysts. Furthermore, the

Journal of Cell Science (2015) 128, 4366-4379 doi:10.1242/jcs.173518

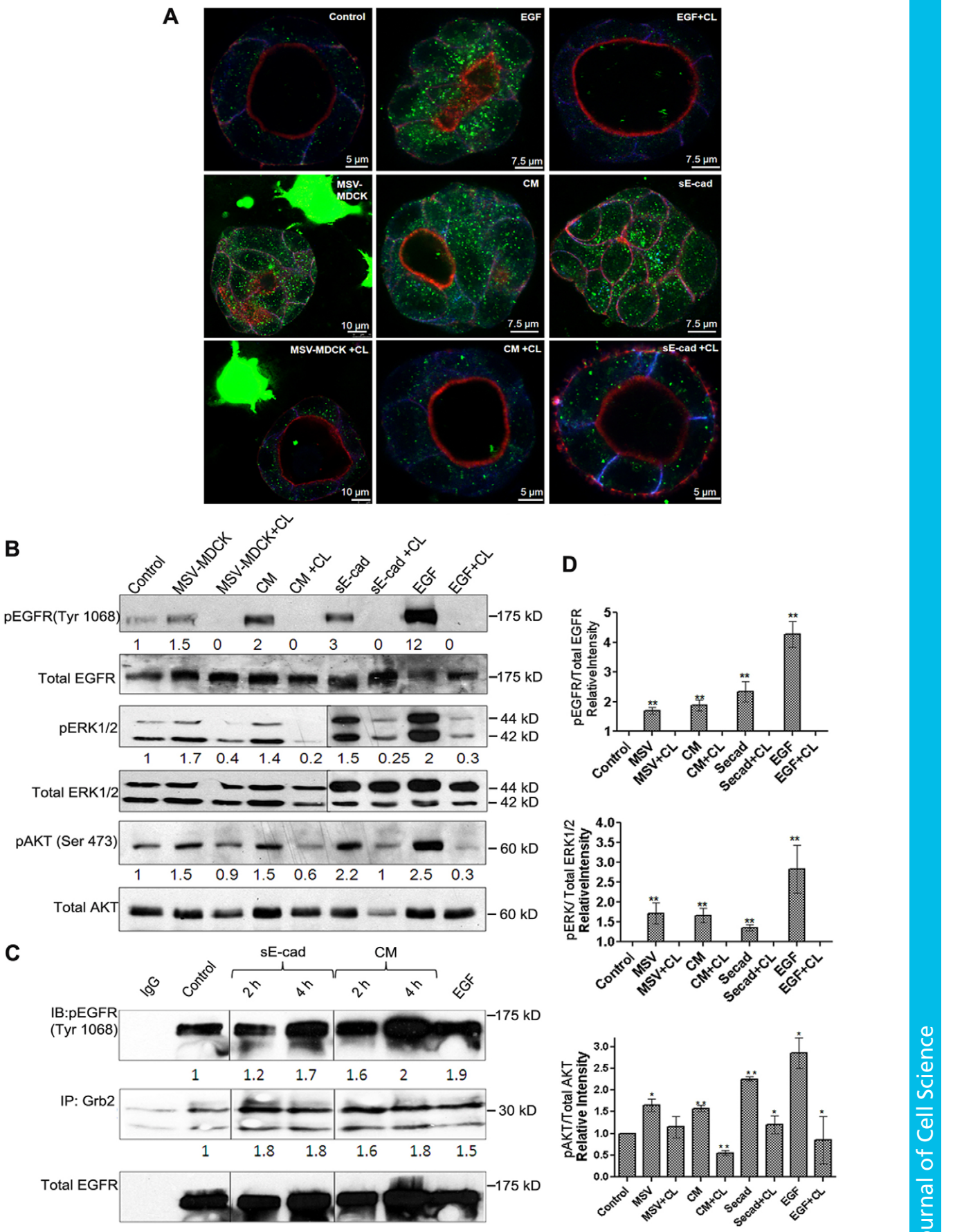

Fig. 4. See next page for legend.

Journal of Cell Science

Journal of Cell Science (2015) 128, 4366-4379 doi:10.1242/jcs.173518

Fig. 4. MSV-MDCK cells induce lumen filling in MDCK cells by sE-cad-mediated activation of EGFR and downstream AKT and ERK1/2 pathways in MDCK cysts. (A) Representative immunofluorescence images showing increased pEGFR expression in MDCK cysts treated with MSV-MDCK cells, conditioned medium (CM), sE-cad, EGF with or without CL-387,785 (CL). Immunofluorescence shows actin (red), E-cadherin (blue) and pEGFR (green). (B) Representative immunoblot from three independent experiments showing pEGFR, total EGFR, phosphoryalted AKT (pAKT), phosphorylated ERK1/2 (pERK1/2) and total AKT and ERK1/2 levels in MDCK 3D cyst lysates co-cultured with MSV-MDCK cells, conditioned medium, sE-cad and EGF for 4 h. 1 µM CL-387,785, an EGFR kinase inhibitor was used to block EGFR activation for 4 h where indicated. EGF treatment was for 15 min. (C) Co-immunoprecipitation of pEGFR (Tyr1068) with Grb2 in MDCK 3D cysts treated with conditioned medium or sE-cad at 2 h and 4 h. (D) Graphs represent quantification data as mean±s.e.m. from three independent experiments. **P*<0.05, ***P*<0.005 (Student's *t*-test).

EGFR kinase inhibitor CL-387,785 reduced the levels of cell proliferation and anti-apoptotic markers in the sE-cad- and conditioned medium-treated MDCK cysts (Fig. 5B). These data suggest that both increased cell proliferation and anti-apoptotic mechanisms are involved in lumen filling induced by sE-cad.

In order to determine the role of downstream ERK1/2 and AKT pathways in lumen filling, conditioned medium or sE-cad-treated cysts were also treated with specific inhibitors of each pathway. Treatment with the inhibitor U0126 against the MEK family proteins (upstream regulators of ERK proteins) suppressed the expression of Ki67 and Bcl2 as revealed by immunofluorescence analysis. Furthermore, lumen filling in conditioned medium or sE-cad-treated cysts was reduced by 60–70% in presence of U0126, suggesting that ERK1/2 has a key role in sE-cad-mediated lumen filling at 24 h. Interestingly, inhibition of PI3K–AKT pathway by LY294002 led to only a 25% reduction in lumen filling compared to conditioned medium and sE-cad-treated cysts at 24 h (Fig. S2A–D). The concentration of U0126 and LY294002 (1 µM) used in the immunofluorescence analysis effectively blocked ERK1/2 and AKT phosphorylation, respectively (Fig. S2E). These results suggest that lumen filling is predominantly driven by the MEK–ERK pathway.

sE-cad and conditioned medium treatment induced EMT in MDCK cysts

Cysts in co-culture for more than 48 h showed striking morphological changes. At 96 h, control cysts remained spherical, whereas conditioned medium and the sE-cad treatment led to more elongated cells emanating from the cysts (Fig. 6A). This observation led us to hypothesize that sE-cad and conditioned medium can

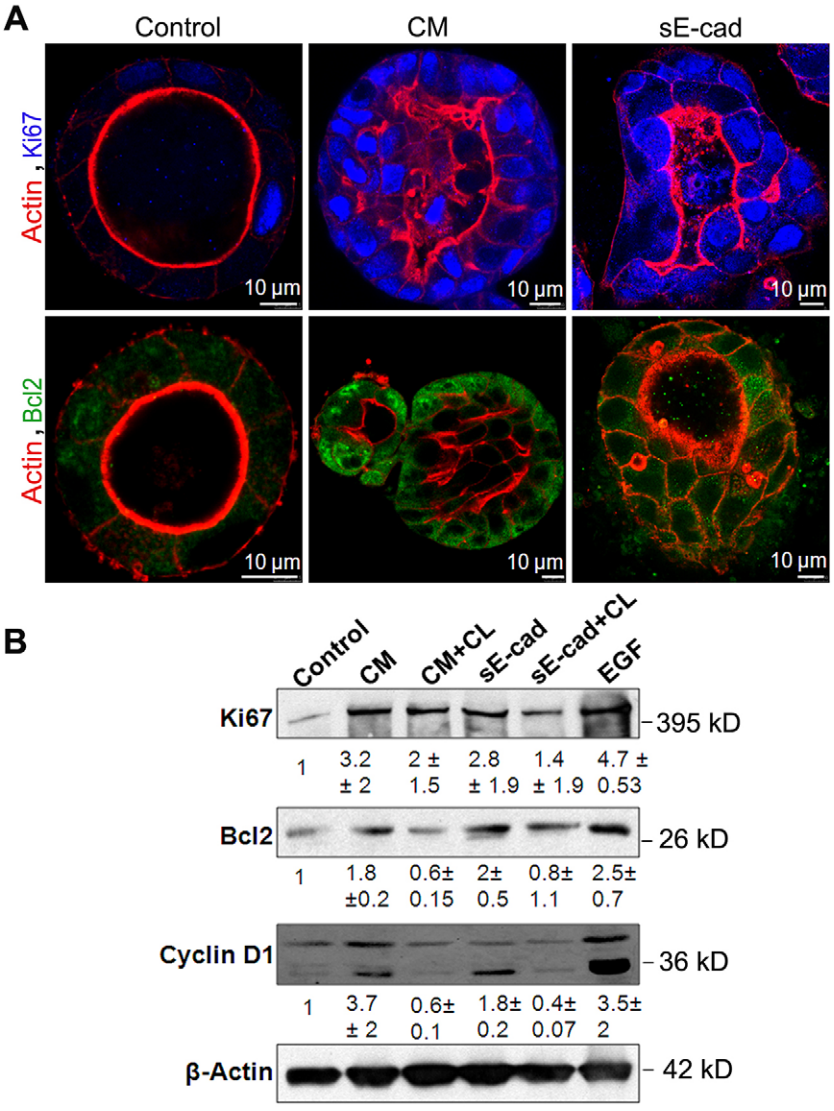

Fig. 5. Lumen filling is a consequence of reduced apoptosis and increased proliferation. (A) Immunofluorescence images showing increased Ki67 and Bcl2 expression in MDCK cysts treated with conditioned medium (CM) and sE-cad for 48 h. Images were obtained from staining cysts with anti-Bcl2 antibody (green), phalloidin–Alexa-Fluor-546 (actin, red) and Ki67 (blue). (B) Representative immunoblot showing Ki67, Bcl2 and cyclin D1 expression in MDCK cysts treated with sE-cad and conditioned medium. 1 µM CL-387,785 (CL) EGFR inhibitor was used where indicated. Quantification data represent mean±s.d. from two independent experiments.

Journal of Cell Science (2015) 128, 4366-4379 doi:10.1242/jcs.173518

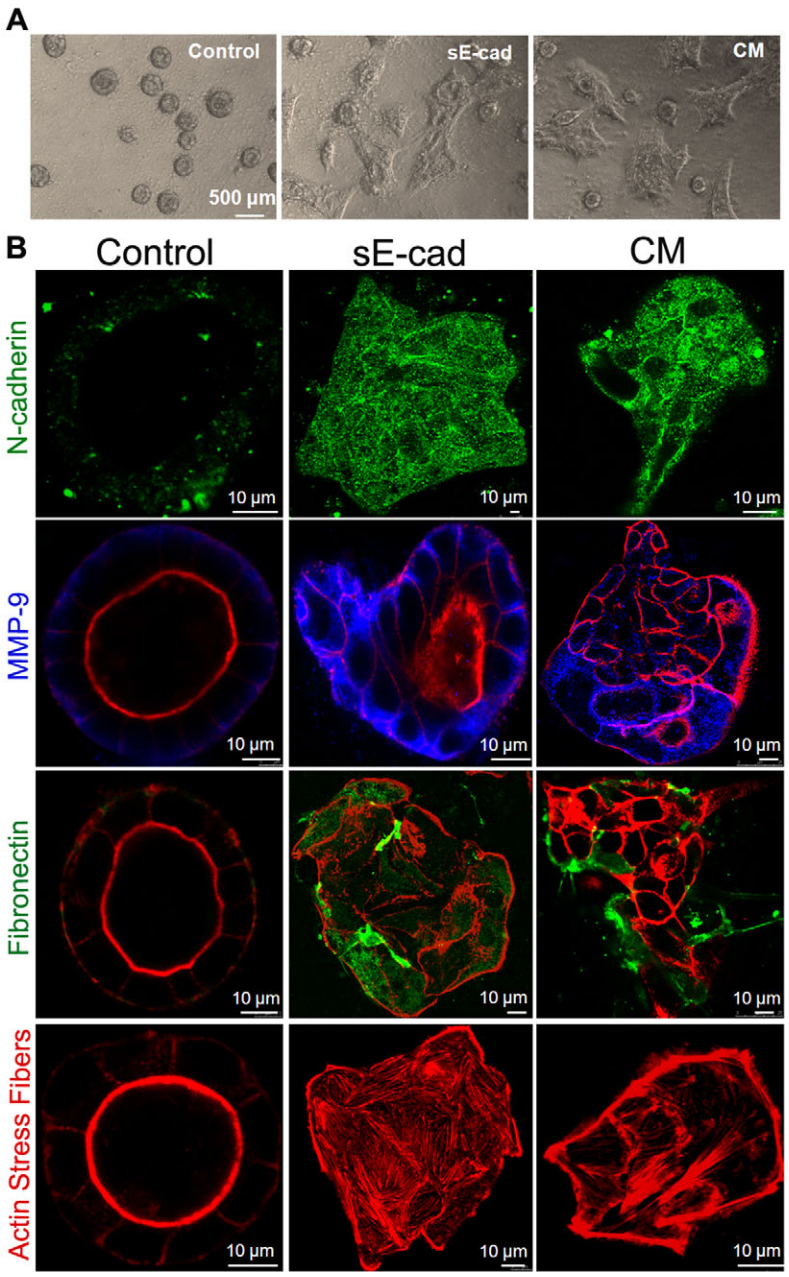

Fig. 6. sE-cad and conditioned medium induces an EMT-like phenotype in MDCK cysts. (A) Phase-contrast images of control MDCK cysts and cysts treated with conditioned medium (CM) and sE-cad for 96 h. (B) Immunofluorescence staining with different EMT markers. Representative merged confocal images showing actin (red), fibronectin (green), N-cadherin (green) and MMP-9 (blue).

induce EMT in the normal epithelial cysts. To confirm EMT, we tested for the presence of multiple EMT markers in the cysts by performing immunofluorescence and immunoblot analyses. As shown in Fig. 6B, the expression of N-cadherin (also known as CDH2), MMP-9 and fibronectin were enhanced in these cells. The presence of stress fibers is a well-established marker for cells undergoing EMT, and is essential for their invasive behavior. Strikingly, enhanced actin stress fibers were detected in the cysts treated with sE-cad and conditioned medium (Fig. 6B). *z*-stacks showing expression of fibronectin, N-cadherin and actin stress fibers in control, sE-cad- and conditioned-medium-treated MDCK cysts for 96 h are shown in Movies 1, 2 and 3 respectively. These results reveal that long-term sE-cad treatment induces EMT in MDCK cysts. It is also important to note that cysts exhibiting an EMT-like phenotype are larger than control cysts.

The PI3K–AKT axis is frequently activated in human cancer and is a key contributor in the induction of EMT (Larue and Bellacosa, 2005). Treatment with the PI3K and AKT inhibitor LY294002 effectively blocked EMT in MDCK cells, with cysts retaining luminal morphology. By contrast, treatment with the MEK inhibitor U0126 did not block EMT in long-term sE-cad- or conditioned-medium-treated cells, as revealed by the expression of fibronectin, N-cadherin and stress fibers using confocal microscopy (Fig. 7A–D). Immunoblot analysis also showed an increase in fibronectin and N-cadherin levels upon sE-cad and conditioned medium treatment, which was blocked in the presence of 1 µM of the PI3K and AKT inhibitor LY294002, but not in the presence of 1 µM MEK inhibitor U0126 (Fig. 7E,F). Long-term inhibition with LY294002 resulted in the inhibition of lumen filling and EMT, possibly by blocking both the PI3K-mediated AKT and ERK pathways. By contrast, long-term treatment with U0126 enhanced the expression of EMT markers in the lumen-filled cysts (Fig. 7A,B); this is because MEK inhibition by U0126 is known to increase AKT activation (Aksamitiene et al., 2010), thereby further

Journal of Cell Science (2015) 128, 4366-4379 doi:10.1242/jcs.173518

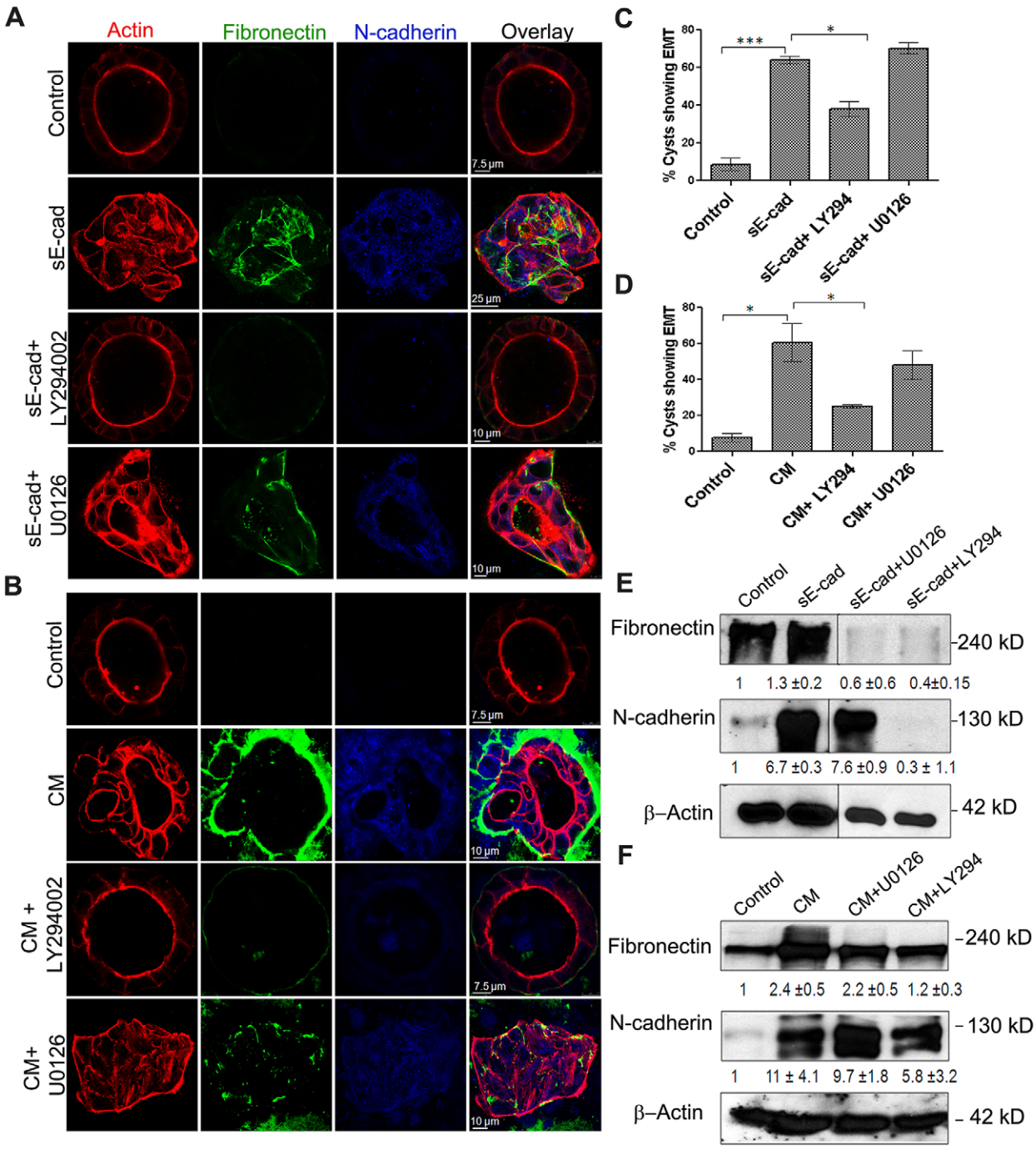

Fig. 7. AKT is involved in the induction EMT in MDCK cysts. (A,B) Immunofluorescence showing EMT expression in cysts treated with sE-cad (A) and conditioned medium (CM; B) in presence of inhibitors at 96 h. U0126 and LY294002 were used at 1 µM each. Representative confocal images obtained from staining cysts with anti-fibronectin antibody (green), anti-N-cadherin antibody (blue), phalloidin–Alexa-Fluor-546 (for actin, red) are shown. (C,D) Quantification of cysts displaying an EMT phenotype after 96 h with sE-cad treatment (C) or conditioned medium treatment (D) in presence of inhibitors. *P<0.05, ***P<0.001 (Student's t-test). (E,F) Representative immunoblots from two independent experiments showing fibronectin and N-cadherin levels in sE-cad-treated cysts (E) and conditioned-medium-treated cysts (F) in the presence of inhibitors. U0126 and LY294002 were used at 1 µM each. β-actin was used as a loading control. Quantification data represent mean±s.d. from two independent experiments.

confirming the role of AKT in driving EMT in MDCK cysts. This is consistent with the immunofluorescence data, which indicates that AKT inhibition blocked EMT more effectively than the MEK–ERK pathway. In addition, long-term treatment with sE-cad revealed distinct activation patterns for ERK and AKT; sE-cad induced ERK activation diminished from 48 to 96 h, whereas the AKT phosphorylation was sustained over 96 h as determined by immunoblot analysis (Fig. S3). These results further authenticate that sustained activation of AKT is involved in the induction of EMT.

DISCUSSION

Normal epithelial cells co-exist with carcinoma cells in solid tumors. Although it is well known that the TME contributes to metastatic

Journal of Cell Science (2015) 128, 4366-4379 doi:10.1242/jcs.173518

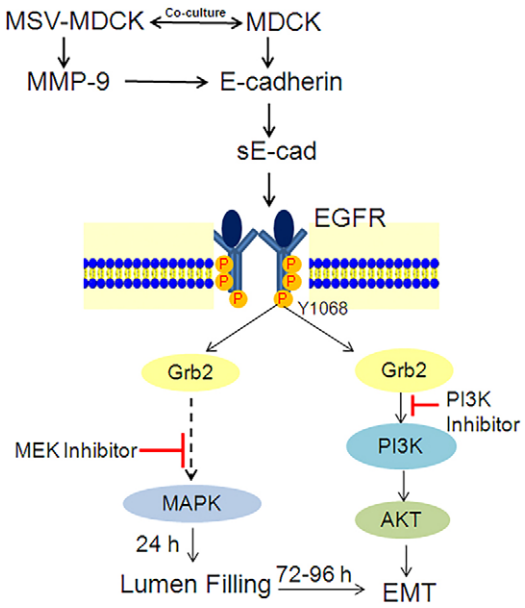

Fig. 8. Proposed model for sequential lumen filling and EMT induced by carcinoma cells in MDCK cysts. See text for details.

dormancy, tumor stability, and progression to invasive and metastatic carcinoma (Taylor et al., 2014), it is not known how carcinoma cells interact with normal epithelial cells in the TME. In this study, we used a 3D co-culture system comprising MDCK and MSV-MDCK cells to address whether carcinoma cells influence adjacent normal epithelial cells. There are many new findings reported here: (1) the development of a co-culture system to study normal and cancer cell interactions; (2) the sequential induction of lumen filling and EMT *in vitro*; (3) that sE-cad acts as a crucial soluble factor involved in the induction of lumen filling and EMT; (4) that carcinoma cells use normal cells as a source for the production of sE-cad; and (5), although, involvement of MMP-9 to cleave E-cadherin, and a role for EGFR in the induction ERK1/2 and AKT signaling pathways has been shown in many cancer cells, we demonstrate that the same well-established oncogenic signaling pathway is utilized by carcinoma cells to induce transdifferentiation of normal cells in the vicinity (Fig. 8). Clinically, these studies suggest that elevated levels of sE-cad present in the sera from cancer patients might have a pathological role in the transdifferentiation of normal epithelial cells, thereby facilitating invasion and metastatic potential.

Filling of the luminal space and multiple lumen lesions are distinctive features of early pre-invasive stages of carcinoma development (Debnath and Brugge, 2005). Several carcinomas such as breast, kidney and prostate carcinomas display lumen filling and architectural disorder during their early stages, before they invade the basement membrane and disseminate (Debnath and Brugge, 2005). The molecular mechanisms that occur during the initial lumen-filling stage of tumorigenesis are poorly understood. A 3D co-culture system comprising epithelial cysts and carcinoma cells is reminiscent of normal epithelial tissue co-existing with tumor cells *in vivo*. This novel 3D assay allowed us to demonstrate that carcinoma cells disrupt epithelial architecture by inducing pre-neoplastic lumen filling. Interference with the key regulators of the apico-basal polarity and tight junction assembly, such as the Crumbs3 and PAR complexes, β1 integrin, RhoA and the Na^+/K^+-ATPase β-subunit generates multiple lumina or no lumen in epithelial cysts (Barwe et al., 2013; Martin-Belmonte et al., 2007; Schluter et al., 2009; Shin et al., 2005; Straight et al., 2004; Yu et al., 2008). However, it is not well known how these markers are affected during carcinogenesis. Our results indicate that carcinoma cells in the vicinity of normal tissue might come in direct physical contact with the normal epithelial cells through filopodia-like projections, or alternatively they might secrete soluble factors that then disrupts luminal architecture. Data obtained using conditioned media strongly suggest that secretion of soluble factors is the primary mechanism by which carcinoma cells induce normal cell transformation. Recent studies have also demonstrated that carcinoma cells induce oncogenic transformation in the adjacent normal epithelial cells using exosomes to force adjacent normal cells to participate in cancer progression (Melo et al., 2014).

A key soluble factor identified in our assay is MMP-9. Although MMP-9 is implicated in the shedding of E-cadherin in several cancer cell lines (Grabowska and Day, 2012), its potential to impact normal cells in the context of the tumor microenvironment has not been examined. Our 3D co-culture system enabled us to determine that MMP-9 released by carcinoma cells acts on E-cadherin on the basolateral surface of adjacent epithelial cells to release sE-cad. Inhibition of MMP-9 abolished sE-cad shedding and consequently blocked the lumen-filling phenotype. Lack of E-cadherin expression on MSV-MDCK cells confirms that the source of sE-cad present in the conditioned medium is primarily from MDCK cells. A transwell co-culture assay involving MCF10A, an immortalized human breast epithelial cell line, with MDA-MB435S, a breast carcinoma cell line lacking E-cadherin expression also revealed MMP-mediated sE-cad shedding from normal cells. This corroborates the finding that tumor cells induce sE-cad shedding from adjacent normal epithelial cells. Although active MMP-2 was also observed in our zymogram, specific inhibition of MMP-9 suggests that MMP-9 plays a prominent role in the production of sE-cad in this co-culture system. However, we cannot rule out the involvement of other MMPs or soluble factors present in the conditioned medium, which might act upstream of MMP-9 and be involved in its activation and the production of sE-cad.

Two complementary approaches were utilized to conclude that sE-cad is essential for the induction of lumen filling and EMT in 3D culture. Exogenously added sE-cad induced lumen filling, whereas, immunodepletion of sE-cad from the conditioned medium blocked the lumen-filling phenotype, indicating that sE-cad is the crucial factor of the conditioned medium that is involved in the induction of lumen filling. Although both purified sE-cad and conditioned medium induced lumen filling, conditioned medium under co-culture conditions might contain additional factors that are not present in the purified sE-cad. These additional factors might be involved in stabilizing or enhancing the effect of sE-cad in conditioned medium. In fact, in co-culture, with conditioned medium the sE-cad levels were 1 µg/ml, which were sufficient to induce lumen filling, indicating that additional factors are likely to be involved. sE-cad has been shown to influence tumor cell proliferation, migration and invasion (Brouxhon et al., 2007; Maretzky et al., 2005; Najy et al., 2008; Noe et al., 2001; Symowicz et al., 2007; Zuo et al., 2011). Here, we show that sE-cad disrupted luminal architecture of fully formed cysts, which was previously unknown. This situation is reminiscent of early tumorigenesis, suggesting that sE-cad in the TME induces a preneoplastic lumen-filling phenotype in adjacent normal epithelial cells.

In polarized epithelial cells, E-cadherin is localized at the adherens junction and along the basolateral region. In our transwell co-culture assay MDCK cells were in the upper chamber and MSV-MDCK cells were in the lower chamber. MMP-9 and sE-cad were only detected in the lower chamber, indicating that the MMP-9 produced by the MSV-MDCK cells cleaved E-cadherin on the basolateral membrane of MDCK cells. MMP-9 inhibition in the

Journal of Cell Science (2015) 128, 4366-4379 doi:10.1242/jcs.173518

lower chamber abrogated sE-cad shedding further confirming this result. Therefore, it is likely that proteases cleave basolaterally localized E-cadherin (David and Rajasekaran, 2012). Additional studies are required to determine whether E-cadherin in adherens junctions is processed by MMP-9.

We demonstrated that the sE-cad-mediated loss of 3D architecture and lumen filling in MDCK cysts is driven by activation of the EGFR and its downstream ERK1/2 and AKT signaling pathways. We showed that co-culture with MSV-MDCK cells, conditioned medium or sE-cad induced lumen filling in an EGFR-dependent manner. Activation of EGFR increased cell proliferation as well as reducing apoptosis, thereby resulting in lumen filling, consistent with previous reports (Reginato et al., 2005).

It has been shown that sE-cad acts as a ligand to the EGFR family of receptors, leading to activation of oncogenic signaling in squamous cell carcinoma cells as well as breast cancer cells (Brouxhon et al., 2014a, 2013a,b; Najy et al., 2008). It should be noted that the cell lines used in these studies were tumor-derived cells. Our co-immunoprecipitation assay reveals that purified sE-cad binds to pEGFR (Tyr1068) in normal epithelial cells. Although this assay is not quantitative, it reveals an association of sE-cad with EGFR. Thus, it seems likely that sE-cad also functions as an EGFR ligand in normal epithelial cells. Interestingly, our cell surface internalization assay reveals that, unlike EGF, internalization of EGFR in the presence of sE-cad is substantially reduced. Endocytosis of EGFR, following ligand binding, functions as a crucial negative regulator of EGFR signaling, particularly EGFR-induced ERK1/2 and AKT signaling (Sousa et al., 2012; Tomas et al., 2014). Interestingly, EGFR mutants present in non-small cell lung cancer display defects in endocytotic regulation, leading to persistent signaling from the plasma membrane (Shtiegman et al., 2007). The differential rate of receptor internalization induced by EGF and sE-cad might be due to faster recycling of EGFR to the membrane upon sE-cad activation thereby resulting in increased stabilization of EGFR at the cell surface. However, additional experiments are needed to validate this notion. Thus, reduction of EGFR internalization in the presence of sE-cad might be one of the mechanisms of EGFR activation in our co-culture model.

Previous reports from our laboratory have demonstrated that sE-cad retains the ability to interact with E-cadherin, and that E-cadherin is necessary for the anti-apoptotic effect of sE-cad in MDCK cells (Inge et al., 2011). E-cadherin homophilic adhesion between adjacent cells transiently activates the EGFR and its downstream PI3K–AKT and ERK1/2 signaling cascades, thereby inducing cell survival and differentiation (Pece and Gutkind, 2000). sE-cad binding to E-cadherin might mimic E-cadherin homophilic binding, resulting in the activation of the EGFR signaling cascade. However, given that the sE-cad–E-cadherin interaction does not result in junction formation and cell adhesion, the subsequent EGFR transactivation might trigger atypical cellular pathways, such as proliferation and survival. Taken together, sE-cad-mediated lumen filling might be a consequence of both sE-cad–E-cad as well as sE-cad–EGFR interactions.

The occurrence of EMT in two-dimensional (2D) cultures is well established. For example, TGFβ induces EMT (Heldin et al., 2009; Kim et al., 2004). However, induction of EMT in 3D epithelial structures has not been shown previously. We demonstrated that long-term treatment of MDCK cysts with sE-cad or conditioned medium induced transdifferentiation of the cysts into a disorganized motile mesenchymal phenotype. Cells with a mesenchymal morphology were observed emanating from the cysts with a consequent loss of cyst morphology. These mesenchymal cells were highly motile. Consistent with their morphology, the mesenchymal markers N-cadherin, fibronectin and actin stress fibers were upregulated. MMP-9 expression was also elevated in these cells. These results indicate that sE-cad produced either directly or indirectly by carcinoma cells can induce EMT in adjacent normal epithelial cells. The trigger that induces EMT following pre-neoplastic lumen filling is not known. Although both AKT and ERK1/2 pathways are activated, inhibition of AKT rather than the ERK1/2 pathway abrogated EMT. Inhibition of ERK1/2 pathway prevented lumen filling effect at 24 h; however, long-term treatment with the MEK inhibitor U0126 resulted in induction of EMT markers and loss of hollow lumen. We hypothesize that the inhibition of the ERK1/2 pathway for 96 h induces compensatory activation of the PI3K–AKT pathway, which drives induction of EMT and disruption of hollow lumen at 96 h. Constitutively active AKT has been reported to drive EMT within 72–96 h (Grille et al., 2003). Here, we have shown the strength of the ERK1/2 signaling reduced after 48 h, whereas AKT phosphorylation was elevated at 72 and 96 h, suggesting that sustained activation of AKT drives induction of EMT in MDCK cysts.

We demonstrated that cancer cells can utilize the surrounding normal epithelial cells as accomplices to produce pro-oncogenic factors. This finding might have important clinical correlations, as our results suggest that elevated sE-cad levels observed in sera from cancer patients are derived from both tumor cells and adjacent normal cells. Carcinoma cells induced shedding of cell bound E-cadherin from adjacent normal tissue and this might influence transdifferentiation of the compact epithelial tissue into a disorganized group of mesenchymal cells. Elevated sE-cad levels might also have pro-tumorigenic effects on other components of the TME, such as the various stromal cell types. Thus, accumulation of sE-cad in the microenvironment might have additive or synergistic effects on the pro-oncogenic TME since it can alter several components of the TME. Disruption of normal epithelial cell function could enhance basal extrusion of tumor cells (Slattum and Rosenblatt, 2014), and thereby accelerate metastasis of the tumor cells.

Blocking sE-cad using a monoclonal antibody (mAb) has been shown to be an effective anti-tumor strategy in mouse models of breast carcinoma and squamous skin carcinoma. Anti-sE-cad mAb treatment attenuates activation of multiple receptor tyrosine kinases such as HER1, HER2 and IGF-1R, and leads to activation of apoptotic pathways and inhibition of proliferative pathways, ultimately attenuating tumor growth in mice (Brouxhon et al., 2014a, 2013a). Although a more detailed analysis examining the toxicity and specificity of anti-sE-cad mAb therapy is necessary, antibody-mediated elimination of sE-cad could act synergistically with current EGFR-based therapies to improve efficacy in the treatment of a range of carcinomas.

MATERIALS AND METHODS

Cell lines

Madin–Darby canine kidney cells (MDCK) and MD-MB-435 S were purchased from the American Type Culture Collection (Manassas, VA) and were maintained in Dulbecco's modified Eagle's medium (DMEM) with 1 g/l sodium bicarbonate, 10% fetal bovine serum, 1 mM L-glutamine, 100 U/ml penicillin and 100 µg/ml streptomycin. MCF-10A cells were also obtained from the American Type Culture Collection and maintained in DMEM with F12 (Gibco-BRL) supplemented with 5% donor horse serum, 20 ng/ml EGF, 10 µg/ml insulin, 100 ng/ml cholera toxin, 0.5 µg/ml hydrocortisone, 50 U/ml penicillin and 50 µg/ml streptomycin. The Moloney-Sarcoma-virus-transformed MDCK cell line (MSV-MDCK) has been described previously (Rajasekaran et al., 2001). Cell lines expressing GFP and RFP were generated by transfection. MDCK epithelial cells stably

Journal of Cell Science (2015) 128, 4366-4379 doi:10.1242/jcs.173518

expressing RFP–actin were used for live microscopy experiments. MSV-MDCK cells expressing GFP were generated as described previously (Barwe et al., 2005).

Antibodies and reagents

Primary antibodies used in this study for immunoblotting and immunostaining were against: E-cadherin (Decma-1; Sigma-Aldrich), MMP-9 (Santa Cruz Biotechnology), Ki67 and N-cadherin (Abcam), fibronectin and β-catenin (BD Transduction Laboratories), smooth muscle actin (Santa Cruz Biotechnology), total EGFR (Fitzgerald Industries), pEGFR (Tyr1068), phosphorylated AKT (Ser473), phosphorylated p44/42 MAPK (ERK1/2), Grb2, total AKT, total MAPK, cyclin D1 and Bcl2 (Cell Signaling Technology). The horseradish peroxidase (HRP)-conjugated anti-mouse-IgG, rabbit-IgG and rat-IgG secondary antibodies were obtained from Cell Signaling Technology. AlexaFluor-488-conjugated anti-mouse-IgG, Alexa-Fluor-633-conjugated anti-rabbit-IgG, Alexa-Fluor-546-conjugated phalloidin and TOPRO-3 were purchased from Molecular Probes. FITC- and Texas-Red-labeled, affinity-purified secondary antibodies were obtained from Jackson ImmunoResearch Laboratories.

Growth-factor-reduced Matrigel™ (Corning Discovery Labware) was used for 3D culture. Protein-free and serum-free UltraDOMA™ medium (Lonza) was used for conditioned medium experiments. Corning cell recovery solution was used to harvest 3D cultures from the Matrigel™ matrix.

The broad spectrum MMP inhibitor Marimastat, and U0126 and LY294002 were purchased from Tocris (Minneapolis, MN). Recombinant human EGF from Peprotech, EGFR Inhibitor CL-387,785 and MMP-9 Inhibitor I (CAS1177749-58-4) were purchased from EMD Millipore Chemicals.

3D Matrigel™ cultures

MDCK 3D cultures were grown and maintained in Matrigel™ as previously described (O'Brien et al., 2001, 2006). Briefly, MDCK cells were trypsinized and suspended at a final concentration of 15,000 cells/ml in 2% growth-factor-reduced Matrigel™. The cell–Matrigel™ mixture (4500 cells per well in 300 µl) was layered onto Matrigel™-coated chambers, 3.5 µl/well, (LAB-TEK II Chambered Coverglass, Nalgene Nunc International) and incubated at 37°C, 5% CO_2 and 95% humidity. Cells were monitored daily for cyst formation. Medium was replenished every 2 days. MDCK cysts grow in 72–96 h. For sE-cad experiments, cysts were cultured with 10 µg/ml of recombinant purified sE-cad in serum-free medium for the indicated time points. For experiments requiring MSV-MDCK co-culture, MSV-MDCK cells (3000 cells per 200 µl) were overlaid onto acini on day 3 of culture and monitored at the indicated time points. Conditioned medium is growth medium from MSV-MDCK cells after 48 h culture. Conditioned medium was centrifuged to remove floating cells and other debris. EGF was used at a concentration of 1 ng/µl wherever indicated.

Purification of sE-cad

sE-cad was purified from the sE-cad-overexpressing HEK-293T cells using Ni-NTA resin as described previously (Inge et al., 2011). Briefly, sE-cad-overexpressing HEK-293T cells were generated by stably expressing the pSEC-Tag2-SECAD vector into HEK-293T cells and stable clones were selected with Zeocin (Invitrogen). sE-cad-HEK-293T cells were grown in Ultra-DOMA-PF (Cambrex, Rutherford, NJ) medium for 48 h. 100 µg/ml of Zeocin antibiotic was added to induce sE-cad expression into the extracellular media. The medium was collected and centrifuged to remove cells and debris. The cell-free growth medium from 48 h was mixed with Ni-NTA resin overnight in a spinner flask to allow the His-tagged sE-cad to bind to the Ni-NTA resin. Resin was then loaded into a column. The resin was washed with 2× column volumes of phosphate buffer (160 mM phosphate, 4 M NaCl, 5 mM Imidazole, pH 7.4), and 5× column volumes of phosphate buffer containing 10 mM imidazole to remove any nonspecific protein. sE-cad was eluted with 5× column volumes of phosphate buffer containing 250 mM imidazole. Fractions (1 ml) were collected and the purity of each fraction was determined by SDS-PAGE. sE-cad-containing fractions were pooled, concentrated using centriplus centrifuge filters (Millipore) and dialyzed against sterile PBS at 4°C. The concentration of the purified sE-cad was determined using a Bio-Rad protein DC kit (Hercules, CA). The purified, concentrated sE-cad was aliquoted and stored at −80°C until further use.

Immunofluorescence of 3D Matrigel™ cultures

Cells grown in Matrigel™ were prepared and immunostained as follows: 3D MDCK cultures were fixed with 4% paraformaldehyde for 15 min at room temperature, washed three times with phosphate-buffered saline (PBS), then permeabilized and blocked with PBS, 0.7% fish skin gelatin and 10% saponin (PFS) for 30 min at room temperature. The fixed and permeabilized cysts were stained for the following proteins: β-catenin, actin, and pEGFR, Ki67, Bcl2, N-cadherin and fibronectin by incubating the antibodies at 1:400 dilution in PFS overnight at 4°C. Staining was detected using Alexa-Fluor-488,546- and 633-conjugated secondary antibodies at 1:400 dilution in PFS and added to cultures for 2 h at room temperature. TOPRO-3 at 1:1000 dilution was used to stain nuclei. Cells and cysts were then washed with PBS three times and used for imaging.

Confocal microscopy and quantification of 3D cysts

Images were captured using a *Leica* TCS SP5 scanning confocal microscope (Leica Microsystems) using a 63×/1.4 NA oil immersion objective lens. The cysts were assessed for the presence of cells within the lumen. The number of cysts with clear or filled lumens were counted across at least ten different random fields and expressed as a percentage of total number of cysts. At least 100 cysts were examined per experimental group. All images were captured using the same laser intensity, and gain and offset settings.

Generating 3D cell lysates and conditioned medium from 3D cultures

3D cyst protein lysates were prepared by recovering cultured cells from the Matrigel™ basement matrix using a cell recovery solution (Corning Life Sciences Product #354253) following the manufacturer's instructions. The harvested cysts were then lysed as described previously (Tushir and D'Souza-Schorey, 2007). Briefly, chilled RIPA buffer (50 mM Tris-HCl pH 7.4, 1% NP-40, 0.5% Na-deoxycholate, 0.1% SDS, 150 mM NaCl and 2 mM EDTA) supplemented with 1× protease inhibitor cocktail and 1% phenylmethylsulfonyl fluoride was added to the harvested cyst pellet. The cells in RIPA buffer were incubated on ice for 15 min followed by sonication for 15 min at 4°C. Lysates were cleared by centrifugation at 16,000 ***g*** for 15 min at 4°C. Supernatants were collected and the protein concentration was measured using Bio-Rad DC reagent as per the manufacturer's instructions. For detection of proteins (shed sE-cad and MMP-9) in the conditioned medium, the cysts were grown in UltraDOMA-PF to prevent interference from albumin and other serum proteins present in the complete medium. Conditioned medium was collected and concentrated using Amicon ultracentrifugation filter devices (EMD, Millipore). Equal amounts of concentrated medium were then loaded onto SDS-polyacrylamide gels and analyzed by immunoblotting or gelatin zymography.

Immunoblotting

SDS-PAGE was used to separate proteins in 3D cyst lysates. Separated proteins were transferred from the gel onto a nitrocellulose membrane. For immunoblotting, the membranes were blocked in 5% non-fat milk in TBS with 0.1% Tween 20 (TBS-T), and then probed with primary antibodies at a dilution of 1:1000 and incubated overnight at 4°C. The membranes were further probed with HRP-conjugated anti-rabbit-IgG, -mouse-IgG or -rat-IgG secondary antibodies diluted 1:2000 in 5% non-fat milk in TBS-T and incubated for 1 h at room temperature. For detection of Ki67 protein (molecular mass, 345–395 kDa), 3–8% Tris acetate (NuPage Novex) gradient gels were used. Antibody binding was visualized using enhanced chemiluminescence (ECL) and ECL prime (GE Healthcare). ImageJ software was utilized for immunoblot quantification and image analysis.

Gelatin zymography

Gelatin zymography was performed as described previously, with modifications (Lu et al., 2004). Samples were mixed with zymogram sample buffer and loaded onto 8% polyacrylamide gels containing 0.1%

gelatin. The gels were run in zymogram running buffer (pH 8.3) without SDS, and then incubated in 1× zymogram renaturation solution for 30 min at room temperature, followed by overnight incubation at room temperature in the zymogram development solution. All the buffers for zymography were purchased from Bio-Rad (Hercules, CA) and used as per the manufacturers' instruction. The gels were stained with Coomassie Brilliant Blue R250 for 2 h at room temperature, and destained until the gelatinolytic activities were detected as clear bands against the blue background.

Transwell co-culture assay

MDCK cells were seeded onto 0.4-µm pore size Transwell filters (Corning Life Sciences) and cultured in a six-well plate. MSV-MDCK carcinoma cells were seeded at increasing densities ranging from 3000–10,000 cells per well in a separate six-well plate. MDCK polarized monolayers (TER >250 ohms/cm^2) on Transwell filters were then transferred onto the MSV-MDCK cells. Co-cultures in the presence and absence of MMP-9 inhibitor were maintained for 48 h in Ultra-DOMA-PF. Growth medium from the lower (basolateral side) and upper (apical side) chambers was used for analyzing MMP-9 and sE-cad levels. MMP-9 activity in the conditioned medium was analyzed using gelatin zymography.

Co-immunoprecipation and immunodepletion

Immunoprecipitation assays were carried out by harvesting cysts from Matrigel™ matrix using cell recovery solution (Corning Lifesciences) and preparing cell lysates using RIPA buffer as described above. Antibodies against pEGFR (Tyr1068), Grb-2, E-cadherin and Myc-tag were pre-coupled to protein G/A agarose beads with rabbit anti-mouse-IgG antibody (RAM) for 4 h and incubated overnight with 1 mg of total protein lysate. The beads were washed and the samples eluted using 4× sample buffer. The samples were separated by SDS-PAGE and immunoblotted to visualize precipitated proteins.

To deplete sE-cad from the co-culture conditioned medium, the conditioned medium was collected and cleared of cells by centrifugation. The conditioned medium was then incubated overnight with anti-E-cadherin antibody coupled to Protein-A–agarose beads. Depletion of sE-cad from conditioned medium was confirmed using SDS-PAGE of conditioned medium samples and the Protein-A–agarose beads. The sE-cad-depleted conditioned medium was then added back to new MDCK cysts to determine its effect on lumen filling.

Biotinylation internalization assay

MDCK cell surface proteins were treated with 0.5 mg/ml cleavable sulfo-NHS-SS-biotin (Pierce) for 30 min at 4°C. After quenching the excess biotin with 50 mM NH_4Cl in PBS containing 0.1 mM $CaCl_2$ and 1 mM $MgCl_2$, the cells were stimulated with 10 µg/ml sE-cad or 10 ng/ml of EGF for 30 min and 60 min at 37°C. For controls, untreated plates were either reduced on ice (reduced) or not reduced. Following treatment, the remaining biotin on the cell surface was stripped with the membrane-impermeant reducing reagent 50 mM MesNa in 100 mM Tris-HCl pH 8.6 (containing 100 mM NaCl and 2.5 mM $CaCl_2$) at 4°C for 30 min. Cells were lysed in 0.5 ml of lysis buffer (10 mM Tris-HCl, 1% Triton X-100, 1 mM EGTA, 1 mM PMSF, 5 mg/ml each of antipain, leupeptin and pepstatin). Protein (500 µg) from each lysate was used for precipitation (16 h at 4°C) with 30 µl of Ultralink streptavidin beads (Pierce) and the precipitates were probed with anti-EGFR and anti-E-cadherin antibody. To calculate the amount of cell surface EGFR, the levels from EGF and sE-CAD-treated samples were calculated with respect to non-reduced controls (100%).

Statistical analysis

Results are expressed as mean±s.e.m. and as mean±s.d., as indicated. Statistical analysis between experimental groups was done using Student's *t*-test and two-way ANOVA. $P<0.05$ was considered significant.

Acknowledgements

We thank Dr Anne Muesch, Albert Einstein Medical College, NY for providing MDCK-RFP cells.

Competing interests

The authors declare no competing or financial interests.

Author contributions

P. U. Patil and A. K. Rajasekaran conceived and designed the work, and with J.D'Ambrosio, developed the methodology. P. U. Patil, J. D'Ambrosio, L. J. Inge and A. K. Rajasekaran acquired data. P. U. Patil, L. J. Inge and A. K. Rajasekaran analyzed and interpreted data (eg. statistical analysis, biostatistics, computational analysis). P. U. Patil, R. W. Mason and A. K. Rajasekaran wrote, review and/or revised the manuscript. R. W. Mason and A. K. Rajasekaran contributed to administrative, technical and material support (ie. reporting or organizing data, constructing databases). A. K. Rajasekaran supervised the study.

Funding

This work was supported by funds from the National Institutes of Health (NIH) [grant number DK56216]; the Nemours Research Programs; and the Centers of Biomedical Research Excellence (COBRE) [grant number P20GM103464]. Deposited in PMC for release after 12 months.

Supplementary information

Supplementary information available online at
http://jcs.biologists.org/lookup/suppl/doi:10.1242/jcs.173518/-/DC1

References

Aksamitiene, E., Kholodenko, B. N., Kolch, W., Hoek, J. B. and Kiyatkin, A. (2010). PI3K/Akt-sensitive MEK-independent compensatory circuit of ERK activation in ER-positive PI3K-mutant T47D breast cancer cells. *Cell Signal.* **22**, 1369-1378.

Barwe, S. P., Anilkumar, G., Moon, S. Y., Zheng, Y., Whitelegge, J. P., Rajasekaran, S. A. and Rajasekaran, A. K. (2005). Novel role for Na,K-ATPase in phosphatidylinositol 3-kinase signaling and suppression of cell motility. *Mol. Biol. Cell* **16**, 1082-1094.

Barwe, S. P., Skay, A., McSpadden, R., Huynh, T. P., Langhans, S. A., Inge, L. J. and Rajasekaran, A. K. (2013). Na,K-ATPase beta-subunit cis homo-oligomerization is necessary for epithelial lumen formation in mammalian cells. *J. Cell Sci.* **125**, 5711-5720.

Behrens, J., Mareel, M. M., Van Roy, F. M. and Birchmeier, W. (1989). Dissecting tumor cell invasion: epithelial cells acquire invasive properties after the loss of uvomorulin-mediated cell-cell adhesion. *J. Cell Biol.* **108**, 2435-2447.

Brouxhon, S., Kyrkanides, S., O'Banion, M. K., Johnson, R., Pearce, D. A., Centola, G. M., Miller, J.-n. N., McGrath, K. H., Erdle, B., Scott, G. et al. (2007). Sequential down-regulation of E-cadherin with squamous cell carcinoma progression: loss of E-cadherin via a prostaglandin E2-EP2 dependent posttranslational mechanism. *Cancer Res.* **67**, 7654-7664.

Brouxhon, S. M., Kyrkanides, S., Teng, X., O'Banion, M. K., Clarke, R., Byers, S. and Ma, L. (2013a). Soluble-E-cadherin activates HER and IAP family members in HER2+ and TNBC human breast cancers. *Mol. Carcinogen.* **53**, 893-906.

Brouxhon, S. M., Kyrkanides, S., Teng, X., Raja, V., O'Banion, M. K., Clarke, R., Byers, S., Silberfeld, A., Tornos, C. and Ma, L. (2013b). Monoclonal antibody against the ectodomain of E-cadherin (DECMA-1) suppresses breast carcinogenesis: involvement of the HER/PI3K/Akt/mTOR and IAP pathways. *Clin. Cancer Res.* **19**, 3234-3246.

Brouxhon, S. M., Kyrkanides, S., Teng, X., Athar, M., Ghazizadeh, S., Simon, M., O'Banion, M. K. and Ma, L. (2014a). Soluble E-cadherin: a critical oncogene modulating receptor tyrosine kinases, MAPK and PI3K/Akt/mTOR signaling. *Oncogene* **33**, 225-235.

Brouxhon, S. M., Kyrkanides, S., Raja, V., Silberfeld, A., Teng, X., Trochesset, D., Cohen, J. and Ma, L. (2014b). Ectodomain-specific E-cadherin antibody suppresses skin SCC growth and reduces tumor grade: A multitargeted therapy modulating RTKs and the PTEN–p53–MDM2 axis. *Mol. Cancer Ther.* **13**, 1791-802.

Bryant, D. M. and Mostov, K. E. (2008). From cells to organs: building polarized tissue. *Nat. Rev. Mol. Cell Biol.* **9**, 887-901.

Chan, A. O.-O., Chu, K.-M., Lam, S.-K., Wong, B. C.-Y., Kwok, K.-F., Law, S., Ko, S., Hui, W.-M., Yueng, Y.-H. and Wong, J. (2003). Soluble E-cadherin is an independent pretherapeutic factor for long-term survival in gastric cancer. *J. Clin. Oncol.* **21**, 2288-2293.

Chattopadhyay, A., Vecchi, M., Ji, Q.-s., Mernaugh, R. and Carpenter, G. (1999). The role of individual SH2 domains in mediating association of phospholipase C-gamma1 with the activated EGF receptor. *J. Biol. Chem.* **274**, 26091-26097.

David, J. M. and Rajasekaran, A. K. (2012). Dishonorable discharge: the oncogenic roles of cleaved E-cadherin fragments. *Cancer Res.* **72**, 2917-2923.

De Wever, O., Derycke, L., Hendrix, A., De Meerleer, G., Godeau, F., Depypere, H. and Bracke, M. (2007). Soluble cadherins as cancer biomarkers. *Clin. Exp. Metastasis* **24**, 685-697.

Debnath, J. and Brugge, J. S. (2005). Modelling glandular epithelial cancers in three-dimensional cultures. *Nat. Rev. Cancer* **5**, 675-688.

Debnath, J., Mills, K. R., Collins, N. L., Reginato, M. J., Muthuswamy, S. K. and Brugge, J. S. (2002). The role of apoptosis in creating and maintaining luminal space within normal and oncogene-expressing mammary acini. *Cell* **111**, 29-40.

Farina, A. R. and Mackay, A. R. (2014). Gelatinase B/MMP-9 in tumour pathogenesis and progression. *Cancers* **6**, 240-296.
Grabowska, M. M. and Day, M. L. (2012). Soluble E-cadherin: more than a symptom of disease. *Front. Biosci. (Landmark Ed)* **17**, 1948-1964.
Grille, S. J., Bellacosa, A., Upson, J., Klein-Szanto, A. J., van Roy, F., Lee-Kwon, W., Donowitz, M., Tsichlis, P. N. and Larue, L. (2003). The protein kinase Akt induces epithelial mesenchymal transition and promotes enhanced motility and invasiveness of squamous cell carcinoma lines. *Cancer Res.* **63**, 2172-2178.
Gumbiner, B., Stevenson, B. and Grimaldi, A. (1988). The role of the cell adhesion molecule uvomorulin in the formation and maintenance of the epithelial junctional complex. *J. Cell Biol.* **107**, 1575-1587.
Hanahan, D. and Coussens, L. M. (2012). Accessories to the crime: functions of cells recruited to the tumor microenvironment. *Cancer Cell* **21**, 309-322.
Heldin, C.-H., Landström, M. and Moustakas, A. (2009). Mechanism of TGF-beta signaling to growth arrest, apoptosis, and epithelial–mesenchymal transition. *Curr. Opin. Cell Biol.* **21**, 166-176.
Hogan, C., Kajita, M., Lawrenson, K. and Fujita, Y. (2011). Interactions between normal and transformed epithelial cells: their contributions to tumourigenesis. *Int. J. Biochem. Cell Biol.* **43**, 496-503.
Inge, L. J., Barwe, S. P., D'Ambrosio, J., Gopal, J., Lu, K., Ryazantsev, S., Rajasekaran, S. A. and Rajasekaran, A. K. (2011). Soluble E-cadherin promotes cell survival by activating epidermal growth factor receptor. *Exp. Cell Res.* **317**, 838-848.
Ivers, L. P., Cummings, B., Owolabi, F., Welzel, K., Klinger, R., Saitoh, S., O'Connor, D., Fujita, Y., Scholz, D. and Itasaki, N. (2014). Dynamic and influential interaction of cancer cells with normal epithelial cells in 3D culture. *Cancer Cell Int.* **14**, 108.
Kajita, M., Hogan, C., Harris, A. R., Dupre-Crochet, S., Itasaki, N., Kawakami, K., Charras, G., Tada, M. and Fujita, Y. (2010). Interaction with surrounding normal epithelial cells influences signalling pathways and behaviour of Src-transformed cells. *J. Cell Sci.* **123**, 171-180.
Katayama, M., Hirai, S., Kamihagi, K., Nakagawa, K., Yasumoto, M. and Kato, I. (1994). Soluble E-cadherin fragments increased in circulation of cancer patients. *Br. J. Cancer* **69**, 580-585.
Kim, E. S., Kim, M. S. and Moon, A. (2004). TGF-beta-induced upregulation of MMP-2 and MMP-9 depends on p38 MAPK, but not ERK signaling in MCF10A human breast epithelial cells. *Int. J. Oncol.* **25**, 1375-1382.
Larue, L. and Bellacosa, A. (2005). Epithelial–mesenchymal transition in development and cancer: role of phosphatidylinositol 3′ kinase/AKT pathways. *Oncogene* **24**, 7443-7454.
Lu, K. V., Jong, K. A., Rajasekaran, A. K., Cloughesy, T. F. and Mischel, P. S. (2004). Upregulation of tissue inhibitor of metalloproteinases (TIMP)-2 promotes matrix metalloproteinase (MMP)-2 activation and cell invasion in a human glioblastoma cell line. *Lab. Invest.* **84**, 8-20.
Maretzky, T., Reiss, K., Ludwig, A., Buchholz, J., Scholz, F., Proksch, E., de Strooper, B., Hartmann, D. and Saftig, P. (2005). ADAM10 mediates E-cadherin shedding and regulates epithelial cell-cell adhesion, migration, and beta-catenin translocation. *Proc. Natl. Acad. Sci. USA* **102**, 9182-9187.
Martin-Belmonte, F., Gassama, A., Datta, A., Yu, W., Rescher, U., Gerke, V. and Mostov, K. (2007). PTEN-mediated apical segregation of phosphoinositides controls epithelial morphogenesis through Cdc42. *Cell* **128**, 383-397.
Melo, S. A., Sugimoto, H., O'Connell, J. T., Kato, N., Villanueva, A., Vidal, A., Qiu, L., Vitkin, E., Perelman, L. T., Melo, C. A. et al. (2014). Cancer exosomes perform cell-independent microRNA biogenesis and promote tumorigenesis. *Cancer Cell* **26**, 707-721.
Najy, A. J., Day, K. C. and Day, M. L. (2008). The ectodomain shedding of E-cadherin by ADAM15 supports ErbB receptor activation. *J. Biol. Chem.* **283**, 18393-18401.
Noe, V., Fingleton, B., Jacobs, K., Crawford, H. C., Vermeulen, S., Steelant, W., Bruyneel, E., Matrisian, L. M. and Mareel, M. (2001). Release of an invasion promoter E-cadherin fragment by matrilysin and stromelysin-1. *J. Cell Sci.* **114**, 111-118.
O'Brien, L. E., Jou, T.-S., Pollack, A. L., Zhang, Q., Hansen, S. H., Yurchenco, P. and Mostov, K. E. (2001). Rac1 orientates epithelial apical polarity through effects on basolateral laminin assembly. *Nat. Cell Biol.* **3**, 831-838.
O'Brien, L. E., Yu, W., Tang, K., Jou, T.-S., Zegers, M. M. P. and Mostov, K. E. (2006). Morphological and biochemical analysis of Rac1 in three-dimensional epithelial cell cultures. *Methods Enzymol.* **406**, 676-691.
Olumi, A. F., Grossfeld, G. D., Hayward, S. W., Carroll, P. R., Tlsty, T. D. and Cunha, G. R. (1999). Carcinoma-associated fibroblasts direct tumor progression of initiated human prostatic epithelium. *Cancer Res.* **59**, 5002-5011.
Orimo, A., Gupta, P. B., Sgroi, D. C., Arenzana-Seisdedos, F., Delaunay, T., Naeem, R., Carey, V. J., Richardson, A. L. and Weinberg, R. A. (2005). Stromal fibroblasts present in invasive human breast carcinomas promote tumor growth and angiogenesis through elevated SDF-1/CXCL12 secretion. *Cell* **121**, 335-348.
Pece, S. and Gutkind, J. S. (2000). Signaling from E-cadherins to the MAPK pathway by the recruitment and activation of epidermal growth factor receptors upon cell-cell contact formation. *J. Biol. Chem.* **275**, 41227-41233.
Rajasekaran, S. A., Palmer, L. G., Quan, K., Harper, J. F., Ball, W. J., Jr., Bander, N. H., Soler, A. P. and Rajasekaran, A. K. (2001). Na,K-ATPase beta-subunit is required for epithelial polarization, suppression of invasion, and cell motility. *Mol. Biol. Cell* **12**, 279-295.
Reginato, M. J., Mills, K. R., Becker, E. B. E., Lynch, D. K., Bonni, A., Muthuswamy, S. K. and Brugge, J. S. (2005). Bim regulation of lumen formation in cultured mammary epithelial acini is targeted by oncogenes. *Mol. Cell. Biol.* **25**, 4591-4601.
Rojas, M., Yao, S. and Lin, Y.-Z. (1996). Controlling epidermal growth factor (EGF)-stimulated Ras activation in intact cells by a cell-permeable peptide mimicking phosphorylated EGF receptor. *J. Biol. Chem.* **271**, 27456-27461.
Schluter, M. A., Pfarr, C. S., Pieczynski, J., Whiteman, E. L., Hurd, T. W., Fan, S., Liu, C.-J. and Margolis, B. (2009). Trafficking of Crumbs3 during cytokinesis is crucial for lumen formation. *Mol. Biol. Cell* **20**, 4652-4663.
Scholzen, T. and Gerdes, J. (2000). The Ki-67 protein: from the known and the unknown. *J. Cell Physiol.* **182**, 311-322.
Shin, K., Straight, S. and Margolis, B. (2005). PATJ regulates tight junction formation and polarity in mammalian epithelial cells. *J. Cell Biol.* **168**, 705-711.
Shtiegman, K., Kochupurakkal, B. S., Zwang, Y., Pines, G., Starr, A., Vexler, A., Citri, A., Katz, M., Lavi, S., Ben-Basat, Y. et al. (2007). Defective ubiquitinylation of EGFR mutants of lung cancer confers prolonged signaling. *Oncogene* **26**, 6968-6978.
Slattum, G. M. and Rosenblatt, J. (2014). Tumour cell invasion: an emerging role for basal epithelial cell extrusion. *Nat. Rev. Cancer* **14**, 495-501.
Sousa, L. P., Lax, I., Shen, H., Ferguson, S. M., De Camilli, P. and Schlessinger, J. (2012). Suppression of EGFR endocytosis by dynamin depletion reveals that EGFR signaling occurs primarily at the plasma membrane. *Proc. Natl. Acad. Sci. USA* **109**, 4419-4424.
Straight, S. W., Shin, K., Fogg, V. C., Fan, S., Liu, C.-J., Roh, M. and Margolis, B. (2004). Loss of PALS1 expression leads to tight junction and polarity defects. *Mol. Biol. Cell* **15**, 1981-1990.
Sturla, L.-M., Amorino, G., Alexander, M. S., Mikkelsen, R. B., Valerie, K. and Schmidt-Ullrichr, R. K. (2005). Requirement of Tyr-992 and Tyr-1173 in phosphorylation of the epidermal growth factor receptor by ionizing radiation and modulation by SHP2. *J. Biol. Chem.* **280**, 14597-14604.
Symowicz, J., Adley, B. P., Gleason, K. J., Johnson, J. J., Ghosh, S., Fishman, D. A., Hudson, L. G. and Stack, M. S. (2007). Engagement of collagen-binding integrins promotes matrix metalloproteinase-9-dependent E-cadherin ectodomain shedding in ovarian carcinoma cells. *Cancer Res.* **67**, 2030-2039.
Takeichi, M. (1991). Cadherin cell adhesion receptors as a morphogenetic regulator. *Science* **251**, 1451-1455.
Taylor, D. P., Clark, A., Wheeler, S. and Wells, A. (2014) Hepatic nonparenchymal cells drive metastatic breast cancer outgrowth and partial epithelial to mesenchymal transition. *Breast Cancer Res. Treat.* **144**, 551-560.
Tiwari, N., Gheldof, A., Tatari, M. and Christofori, G. (2012). EMT as the ultimate survival mechanism of cancer cells. *Semin. Cancer Biol.* **22**, 194-207.
Toillon, R.-A., Chopin, V., Jouy, N., Fauquette, W., Boilly, B. and Le Bourhis, X. (2002). Normal breast epithelial cells induce p53-dependent apoptosis and p53-independent cell cycle arrest of breast cancer cells. *Breast Cancer Res. Treat.* **71**, 269-280.
Tomas, A., Futter, C. E. and Eden, E. R. (2014). EGF receptor trafficking: consequences for signaling and cancer. *Trends Cell Biol.* **24**, 26-34.
Tushir, J. S. and D'Souza-Schorey, C. (2007). ARF6-dependent activation of ERK and Rac1 modulates epithelial tubule development. *EMBO J.* **26**, 1806-1819.
Yarden, Y. (2001). The EGFR family and its ligands in human cancer: signalling mechanisms and therapeutic opportunities. *Eur. J. Cancer* **37** Suppl. 4, 3-8.
Yu, W., Shewan, A. M., Brakeman, P., Eastburn, D. J., Datta, A., Bryant, D. M., Fan, Q.-W., Weiss, W. A., Zegers, M. M. P. and Mostov, K. E. (2008). Involvement of RhoA, ROCK I and myosin II in inverted orientation of epithelial polarity. *EMBO Rep.* **9**, 923-929.
Zegers, M. M. P., O'Brien, L. E., Yu, W., Datta, A. and Mostov, K. E. (2003). Epithelial polarity and tubulogenesis in vitro. *Trends Cell Biol.* **13**, 169-176.
Zuo, J.-H., Zhu, W., Li, M.-Y., Li, X.-H., Yi, H., Zeng, G.-Q., Wan, X.-X., He, Q.-Y., Li, J.-H., Qu, J.-Q. et al. (2011). Activation of EGFR promotes squamous carcinoma SCC10A cell migration and invasion via inducing EMT-like phenotype change and MMP-9-mediated degradation of E-cadherin. *J. Cell Biochem.* **112**, 2508-2517.